

## МОДЕЛИРОВАНИЕ ХИМИЧЕСКОГО СОСТОЯНИЯ ПОВЕРХНОСТИ МИШЕНИ В СИМР С ГОРЯЧЕЙ МИШЕНЬЮ

А.В. Казиев, Д.В. Колодко, А.В. Тумаркин, М.М. Харьков, В.Ю. Лисенков

Андрей Викторович Казиев (ORCID 0000-0001-7411-5570)\*, Александр Владимирович Тумаркин (ORCID 0000-0002-4648-2338), Максим Михайлович Харьков (ORCID 0000-0003-1042-1469), Владислав Юрьевич Лисенков (ORCID 0000-0003-3626-7797)

Кафедра физики плазмы, Национальный исследовательский ядерный университет «МИФИ», Каширское шоссе, 31, Москва, Российская Федерация, 115409  
E-mail: kaziev@plasma.mephi.ru

Добрыня Вячеславич Колодко (ORCID 0000-0002-5043-9922)

Кафедра физики плазмы, Национальный исследовательский ядерный университет «МИФИ», Каширское шоссе, 31, Москва, Российская Федерация, 115409

Институт радиотехники и электроники им. Котельникова РАН, Фрязинский филиал, пл. Введенского, 1, Фрязино, Российская Федерация, 141190

*Теоретически рассмотрено совместное влияние эффектов горячей мишени и импульсного характера разряда на состояние поверхности мишени. Система уравнений описывает состояние мишени посредством значений доли отправленной площади  $\theta_1$  и  $\theta_2$ , где индекс 1 соответствуетmonoатомномуповерхностномуслою, а индекс 2 - слою под поверхностью (приповерхностному слою). Рассмотрены процессы хемосорбции на поверхности мишени и подложки, распыления атомов химически активного газа из мишени, имплантации ионов химически активного газа в приповерхностный слой, испарения материала и переноса между слоями. Отдельное уравнение связывает атомные потоки химически активного газа на поверхностях мишени и подложки с объемными характеристиками, такими как скорость напекания газа и скорость откачки. Система уравнений решена численно, и представлены тестовые результаты. Вычислены зависимости от времени доли химического соединения на поверхности и в приповерхностных слоях мишени, а также на поверхности подложки, в процессе импульсного магнетронного распыления высокой мощности с неохлаждаемой мишенью. Повторяющийся характер СИМР был учтен заданием тока в виде прямоугольных импульсов длительностью 50–500 мкс с частотой 0,1–1 кГц. Модель предсказывает сильное влияние начальных условий отправления мишени на ход процесса распыления на временном масштабе 20 мс. Показано, что степени отправления поверхностей мишени и подложки характеризуются колебаниями с повышенной амплитудой при увеличении паузы между импульсами, даже если коэффициент заполнения остается постоянным.*

**Ключевые слова:** магнетронный разряд, СИМР, распыление, испарение, отправление мишени, COMSOL Multiphysics

### Для цитирования:

Казиев А.В., Колодко Д.В., Тумаркин А.В., Харьков М.М., Лисенков В.Ю. Моделирование химического состояния поверхности мишени в СИМР с горячей мишенью. *Изв. вузов. Химия и хим. технология.* 2023. Т. 66. Вып. 12. С. 76–81. DOI: 10.6060/ivkkt.20236612.6879.

### For citation:

Kaziev A.V., Kolodko D.V., Tumarkin A.V., Kharkov M.M., Lisenkov V.Yu. Simulation of target surface chemical state in a hot-target HiPIMS process. *ChemChemTech [Izv. Vyssh. Uchebn. Zaved. Khim. Khim. Tekhnol.]*. 2023. V. 66. N 12. P. 76–81. DOI: 10.6060/ivkkt.20236612.6879.

## SIMULATION OF TARGET SURFACE CHEMICAL STATE IN A HOT-TARGET HIPIMS PROCESS

**A.V. Kaziev, D.V. Kolodko, A.V. Tumarkin, M.M. Kharkov, V.Yu. Lisenkov**

Andrey V. Kaziev (ORCID 0000-0001-7411-5570)\*, Alexander V. Tumarkin (ORCID 0000-0002-4648-2338), Maksim M. Kharkov (ORCID 0000-0003-1042-1469), Vladislav Yu. Lisenkov (ORCID 0000-0003-3626-7797)

National Research Nuclear University “MEPhI”, Kashirskoe shosse, 31, Moscow, 115409, Russia  
E-mail: kaziev@plasma.mephi.ru\*

Dobrynya V. Kolodko (ORCID 0000-0002-5043-9922)

National Research Nuclear University “MEPhI”, 31 Kashirskoe shosse, 31, Moscow, 115409, Russia  
Kotelnikov Institute of Radio Engineering and Electronics of the RAS, Fryazino Branch, Vvedenskogo pl., 1, Fryazino, 141190, Russia

*We theoretically consider the joint influence of hot-target effects and the pulsed nature of the discharge on the state of the target surface. The system of equations describes the state of the target in terms of poisoned area fractions  $\theta_1$  and  $\theta_2$ , where index 1 corresponds to the monoatomic surface layer, and index 2 - to the layer beneath the surface (subsurface layer). The processes of chemisorption on target and substrate surfaces, sputtering of reactive gas atoms from target, implantation of reactive gas ions to the sub-surface layer, material evaporation, and transfer between the layers are considered. A separate equation connects the atomic fluxes of reactive gas associated with target and substrate surfaces with the volumetric characteristics, such as gas injection rate and pumping speed. The system of equations is solved numerically, and test results are presented. Temporal evolutions of the compound fraction of target surface and subsurface layers as well as the substrate surface in a high-power impulse magnetron sputtering process with uncooled target have been studied numerically. The repetitive fashion of HiPIMS process has been taken into account by introducing current waveform in the shape of rectangular pulses with 50–500  $\mu$ s duration and 0.1–1 kHz frequency. The model predicts strong influence of initial target poisoning conditions on the behavior of sputtering process on the timescale of 20 ms. The compound fractions on target and substrate surfaces demonstrate larger magnitude of oscillations when increasing the pulse-off period, even if the duty factor remains constant.*

**Key words:** magnetron discharge, HiPIMS, sputtering, evaporation, target poisoning, COMSOL Multiphysics

### INTRODUCTION

Magnetron sputtering is one of the most widely used methods of thin solid films preparation for both industrial and research purposes [1-3]. In comparison to other major PVD methods (arc and electron beam evaporation), magnetron sputter deposition is generally characterized by higher density of produced coatings and better adhesion. This is mostly due to higher energy of sputtered particles ( $\sim 10$  eV) than the evaporated ones ( $\sim 0.1$  eV). Further improvement of coating properties can be obtained by utilizing high-power impulse magnetron sputtering with short ( $< 100$   $\mu$ s, HiPIMS [4]) or long (up to 20 ms, L-HiPIMS [5]) pulse duration instead of conventional direct current (DC) or mid-frequency (MF) modes. In this case, high peak power is applied to the target in a pulsed fashion, and plasma density is greatly enhanced, resulting in large fraction of ionized particle flux to the substrate. Unlike

neutral flux, characteristics of the ionized flux can be precisely controlled to tailor the anticipated film structure and functional properties [6].

On the other hand, deposition rates in magnetrons are much lower than in evaporation devices, while in HiPIMS modes they are even lower than in DC/MF. A promising attempt to combine the presence of the group of fast sputtered species, high plasma ionization degree, and high deposition rates of evaporators is to implement impulse magnetron sputtering with uncooled (hot) target [7, 8]. This method is based on magnetron target heating (for some materials, above melting point) by ion flux from plasma thus producing large evaporative flux in addition to the flux of sputtered atoms. In presence of high-power pulses, evaporated and sputtered target material becomes effectively ionized.

Deposition of single-material films in hot-target magnetrons has been studied in a number of recent papers, including Sn, Cu, Cr, Si, Ni, Fe, Ge, Ti [9-26].

It has been demonstrated that the deposition rates in hot-target magnetrons can be several-to-tens times higher than in conventional ones depending on the material. However, even greater interest lies in utilizing this method for preparation of compound films, especially oxides and nitrides. The processes of obtaining oxide and nitride coatings in magnetron sputtering systems are associated with known effects of complex nonlinear and often unstable behavior of the deposition rate and film stoichiometry depending on the reactive gas flow. Theoretical description of reactive magnetron sputtering process was given in a number of seminal papers [27-29], and reliable calculations can be made using these models. However, only few studies exist on uncooled target behavior in reactive sputtering conditions [30-34], and none of the existing models takes into account both time-dependent nature of pulsed discharge parameters and the target surface poisoning and heating effects. We therefore aim at developing such an extended model that could eventually be applied to predict the properties of hot-target reactive HiPIMS discharge modes. Here, we numerically study the chemical state of the target in case of applying a train of high-current discharge pulses.

#### MODELING APPROACH

To build the model, we use similar main assumptions and general approach that we describe in the study of reactive MPPMS process [35]. In its turn, they are largely based on the original steady-state Berg model [28]. The concept is to write the equations for surface area fractions covered with compound (so-called poisoned fractions)  $\theta_i$  of target and substrate/wall surfaces that change in time due to various processes. Here  $i = 1$  stands for monoatomic target surface layer,  $i = 2$  for the layer beneath the surface (subsurface layer), and  $i = 3$  for the substrate/wall surface. The system is then closed by the balance equation for reactive gas species flow in vacuum chamber. Here, we consider the change of poisoned area fractions due to processes of chemisorption on target and substrate surfaces (index "chem"), sputtering of reactive gas atoms from target (index "sput"), implantation of reactive gas ions into the sub-surface layer (index "impl"), target material evaporation (index "evap-m"), evaporation of compound species from target (index "evap-c"), knock-in events with reactive gas atoms (index "k") and their backward transport between the target layers (index "tr").

Transport paths of reactive gas species due to the considered processes are illustrated in Fig. 1 with respect to the structure of target surface layers and substrate/wall surface.

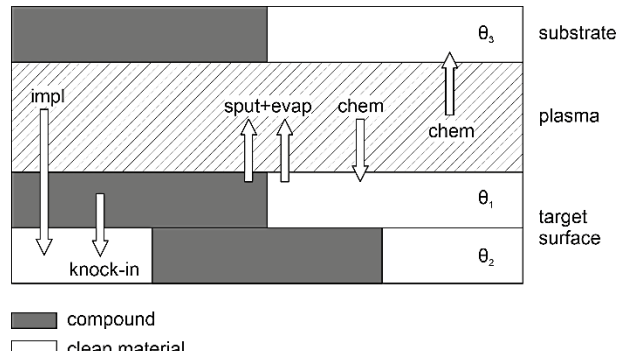


Fig. 1. Transport paths of reactive gas species to and from the target and substrate/wall surfaces

Рис. 1. Пути переноса частиц реакционного газа между поверхностями мишени и подложки/стенок

In the described terms, the system of equations is written as

$$\dot{\theta}_1 = \dot{\theta}_1^{\text{chem}} - \dot{\theta}_1^{\text{sput}} - \dot{\theta}_1^k - \dot{\theta}_1^{\text{evap-c}} + \dot{\theta}_1^{\text{evap-m}} + \dot{\theta}_1^{\text{tr}}, \quad (1)$$

$$\dot{\theta}_2 = \dot{\theta}_2^{\text{impl}} + \dot{\theta}_1^k - \dot{\theta}_1^{\text{tr}}, \quad (2)$$

$$p_{\text{atm}} q = \left( \dot{\theta}_1^{\text{chem}} A_t + \dot{\theta}_3^{\text{chem}} A_s - \dot{\theta}_1^{\text{sput}} A_t - \dot{\theta}_1^{\text{tr}} A_t + \dot{\theta}_2^{\text{impl}} A_t \right) \frac{\xi}{A_{\text{cell}}} + pS, \quad (3)$$

where  $p_{\text{atm}}$  – atmospheric pressure,  $\xi = V_M p_{\text{atm}} / N_A$  – flow unit conversion factor ( $V_M$  – molar volume of gas,  $N_A$  – Avogadro constant),  $A_t$  – target surface area,  $A_s$  – substrate surface area,  $A_{\text{cell}} = K \times (M/\rho N_A)^{2/3}$  is the effective area occupied by a single metal atom of target surface ( $K$  – fit parameter that depends on the surface state,  $M$  – molar mass,  $\rho$  – density),  $p$  – reactive gas pressure  $S$  – pumping speed.

Eq. (1) describes compound formation on the target surface. Eq. (2) describes the conditions in subsurface layer. The balance of reactive gas atoms in the chamber is determined by Eq. (3).

The terms in the right parts of Eqs. (1-3) are written in the following forms:

- $\dot{\theta}_1^{\text{chem}} = k [T_t] v [T_t]^{n/2m} (1 - \theta_1) A_{\text{cell}}$  –

describes compound formation (chemisorption) on the target surface;

- $\dot{\theta}_3^{\text{chem}} = k [T_s] v [T_s]^{n/2m} (1 - \theta_3) A_{\text{cell}}$  –

describes compound formation (chemisorption) on the substrate surface;

- $\dot{\theta}_1^{\text{sput}} = \frac{j}{e} \gamma_c \theta_1 A_{\text{cell}}$  – describes reactive gas species sputtering from the target surface;

•  $\dot{\theta}_1^k = \frac{1}{Z} \frac{j}{e} \gamma_k \theta_1$  – describes knock-in of reactive gas atoms from surface to subsurface layer;

- $\dot{\theta}_1^{\text{evap-c}} = \frac{10^{A_c - B_c/T_t}}{\sqrt{2\pi m_c k_B T_t}} (1 - \theta_1)(1 - \theta_2) A_{\text{cell}}$  –

describes evaporation of compound species from target;

- $\dot{\theta}_1^{\text{evap-m}} = \frac{10^{A_m - B_m/T_t}}{\sqrt{2\pi m_m k_B T_t}} (1 - \theta_1) \theta_2 A_{\text{cell}}$

describes evaporation of target material species;

- $\dot{\theta}_1^{\text{tr}} = \frac{1}{Z} \frac{j}{e} \theta_2 (\gamma_{\text{mm}} (1 - \theta_1) + \gamma_{\text{mc}} \theta_1) A_{\text{cell}}$

describes transfer of reactive gas atoms between layers.

In the equations above  $T_t$  – target temperature,  $T_s$  – substrate temperature,  $k[T_t]$  is the rate coefficient of chemical reaction on the target surface,  $v[T_t]$  is the target surface fraction covered by physically adsorbed reactive gas,  $k[T_s]$  is the reaction rate,  $v[T_s]$  is the substrate surface fraction covered by physically adsorbed reactive gas,  $j$  – ion current density,  $p$  – reactive gas pressure,  $\gamma_c$  – partial sputter yield of gas atoms from compound,  $\gamma_{\text{mc}}$  – partial sputter yield of metal atoms from compound,  $\gamma_{\text{mm}}$  – sputter yield of metal atoms from metal surface,  $\gamma_k$  – knock-in yield,  $e$  – elementary charge,  $k_B$  – Boltzmann constant,  $m_c$  – mass of compound molecule,  $m_m$  – mass of target material atom,  $A_c$ ,  $B_c$ ,  $A_m$ ,  $B_m$  – constants.  $Z$  is the stoichiometry factor of compound, i. e. number of reactive atoms per target material atom in the compound.

We simulate the temporal evolution of the poisoned fractions of target surface and subsurface layers as well as the substrate surface. Numerical studies made for single impulses show that the solutions are extremely sensitive to the initial conditions imposed on  $\theta_1$  and  $\theta_2$ . Therefore, in order to adequately describe the deposition process, one has to take into account the repetitive fashion of voltage and current pulses applied to the target. In our case, the simulations were made for frequencies 1-10 kHz, and pulse width values 10-100  $\mu$ s. The duty cycle is therefore 10%.

## RESULTS AND DISCUSSION

Several combinations of initial conditions have been considered. One can suggest two extreme case of target surface state. The first is clean metallic surface with  $\theta_1 = \theta_2 = 0$ . The second is completely poisoned surface, with compound fractions  $\theta_1 = \theta_2 = 1$ . Together with  $\theta_1$  and  $\theta_2$ , we calculate separate contributions of fluxes of reactive species that correspond to sputtering, knocking-in, implantation, gas supply, and vacuum pumping.

For simplicity, the discharge current was represented as a sequence of rectangular pulses. The repetition frequency  $f$  was 1 kHz, and the pulse-on time  $\tau$  was 50, 200, and 500  $\mu$ s. Reactive gas flow rate was fixed at 30 sccm, which is reasonable for our experimental equipment. Argon pressure was constant and equal to 0.5 Pa.

Obtained temporal dependences of  $\theta_1$ ,  $\theta_2$ ,  $\theta_3$ , and reactive gas pressure for the first 10 discharge

pulses together with discharge current waveform used for simulation ( $f = 1$  kHz,  $\tau = 200 \mu$ s) for initial conditions  $\theta_1^{(0)} = \theta_2^{(0)} = 0$  are shown in Fig. 2.

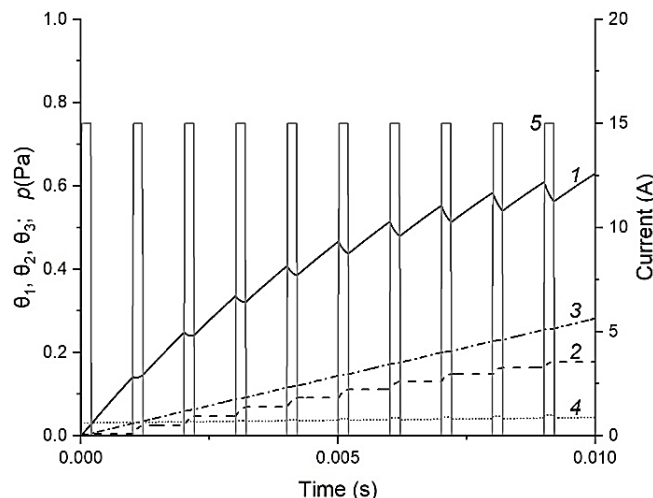


Fig. 2. Time dependences of  $\theta_1$  (1),  $\theta_2$  (2),  $\theta_3$  (3), and reactive gas pressure (4) for the first 10 discharge pulses together with discharge current waveform used for simulation ( $f = 1$  kHz,  $\tau = 200 \mu$ s).

Initial conditions  $\theta_1^{(0)} = \theta_2^{(0)} = 0$

Рис. 2. Временные зависимости  $\theta_1$  (1),  $\theta_2$  (2),  $\theta_3$  (3) и давления реакционного газа (4) для первых 10 разрядных импульсов, а также осциллограмма тока, использованная при моделировании ( $f = 1$  кГц,  $\tau = 200$  мкс). Начальные условия  $\theta_1^{(0)} = \theta_2^{(0)} = 0$

Within the pulse, due to sputtering and evaporation processes, the surface layer becomes depleted of reactive gas species, and  $\theta_1$  decreases accordingly. On the contrary, subsurface layer is supplied with reactant due to ion implantation and knocking-in of atoms from the surface compound layer, and  $\theta_1$  increases in the pulse-on phase. In the pulse-off period characterized by zero discharge current,  $\theta_1$  grows because of continuous chemisorption, while  $\theta_2$  is constant.

Typical results of calculations for comparatively large-scale discharge pulse train (200 pulses) are shown in Fig. 3.

We observe that despite substantial difference in behavior of  $\theta_1$  and  $\theta_2$  curves in the beginning of pulsing for different initial conditions, their steady state value are the same. Eventually, reactive gas pressure reaches level of 0.5 Pa, which is expected for non-reactive gas having the same flow rate. The time of stabilization has an order of 50 ms. However, the difference in dynamics is prominent during some first 20 ms, and this timescale is important for long-pulse HiPIMS and MPPMS modes.

The results of  $\theta_1$  and  $\theta_2$  dynamics obtained for initially poisoned target surface  $\theta_1^{(0)} = \theta_2^{(0)} = 1$  and different temporal parameters of the discharge pulse are shown in Fig. 4. The discharge current is constant  $I = 15$  A.

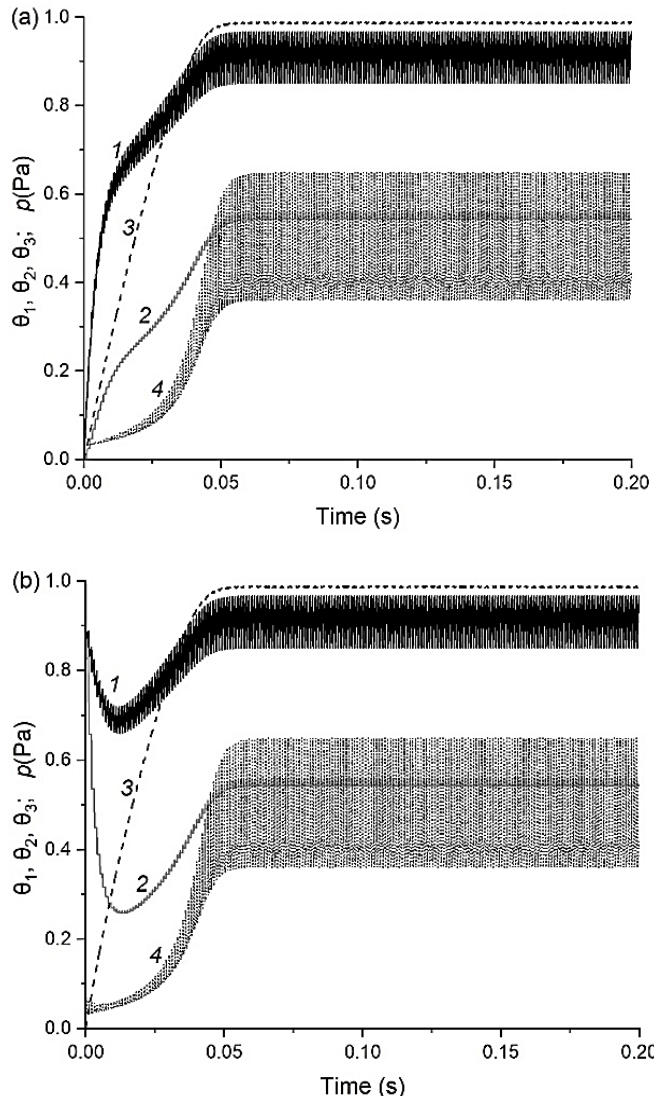


Fig. 3. Time dependences of poisoned fractions  $\theta_1$  (1),  $\theta_2$  (2),  $\theta_3$  (3), and reactive gas pressure (4) for different initial conditions:  
(a)  $\theta_1^{(0)} = \theta_2^{(0)} = 0$ ; (b)  $\theta_1^{(0)} = \theta_2^{(0)} = 1$

Рис. 3. Временные зависимости  $\theta_1$  (1),  $\theta_2$  (2),  $\theta_3$  (3) и давления реакционного газа (4) для разных начальных условий:  
(a)  $\theta_1^{(0)} = \theta_2^{(0)} = 0$ ; (b)  $\theta_1^{(0)} = \theta_2^{(0)} = 1$

The data for  $f = 1$  kHz and different  $\tau$  values demonstrate great influence of pulse-on time on chemical state of both surface and subsurface layers. Longer discharge pulses at fixed repetition frequency result in larger integral sputtering of reactive species that means lower steady-state values of  $\theta_1$  and  $\theta_2$ . Comparison of cases with  $f = 1$  kHz,  $\tau = 50$   $\mu$ s and  $f = 0.1$  kHz,  $\tau = 500$   $\mu$ s, which have the same duty factor  $\tau \times f = 5\%$ , demonstrates that longer pulse-off period (10 ms), or simply, pause between the pulses, triggers oscillations of compound fraction with considerably high magnitude. Presumably, this effect should stimulate arcing on the target and discharge instability, which, however, need experimental verification.

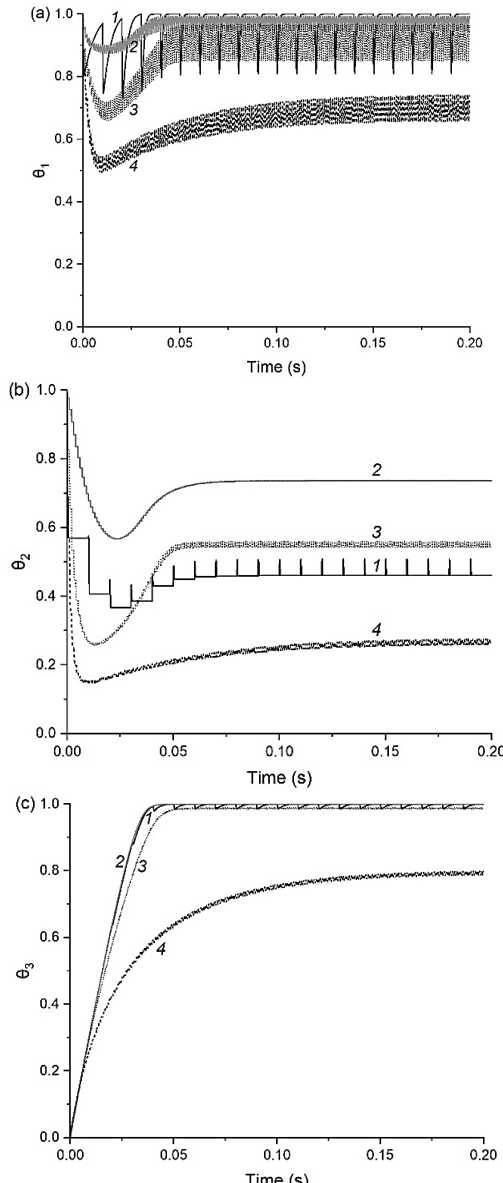


Fig. 4. Temporal evolution of poisoned fractions  $\theta_1$  (a),  $\theta_2$  (b), and  $\theta_3$  (c) for different combinations of pulse-on time and repetition frequency: 1 –  $f = 0.1$  kHz,  $\tau = 500$   $\mu$ s; 2 –  $f = 1$  kHz,  $\tau = 50$   $\mu$ s; 3 –  $f = 1$  kHz,  $\tau = 200$   $\mu$ s; 4 –  $f = 1$  kHz,  $\tau = 500$   $\mu$ s

Рис. 4. Изменение во времени долей отравления  $\theta_1$  (a),  $\theta_2$  (b) и  $\theta_3$  (c) для разных комбинаций значений длительности импульса и частоты повторения: 1 –  $f = 0.1$  кГц,  $\tau = 500$  мкс; 2 –  $f = 1$  кГц,  $\tau = 50$  мкс; 3 –  $f = 1$  кГц,  $\tau = 200$  мкс; 4 –  $f = 1$  кГц,  $\tau = 500$  мкс

## CONCLUSIONS

Reactive HiPIMS process in the pulsed mode can be described by solving a system of developed model equations for periodic discharge current conditions. For a given set of parameters relevant to the experiments, the model predicts strong influence of initial poisoning conditions on the behavior of sputtering process on the timescale of 20 ms. The compound fraction on substrate surface can be controlled by changing the pulse-on time, which is in qualitative agreement with experiment. Increasing pulse-off time at fixed

duty factor results in large oscillations of target surface compound fraction and can compromise the process stability. Nevertheless, these findings require accurate comparison with relevant experiments.

However, a number of phenomena important for hot-target magnetrons have not been included in the model yet. Specifically, combination of melted and solid material in the target and temporal properties of reactant release from subsurface layer should be taken into account.

#### ACKNOWLEDGMENT

*The work was supported by the Russian Science Foundation (grant no. 18-79-10242).*

*The authors declare the absence a conflict of interest warranting disclosure in this article.*

*Работа выполнена при поддержке Российского научного фонда (грант № 18-79-10242).*

*Авторы заявляют об отсутствии конфликта интересов, требующего раскрытия в данной статье.*

#### REFERENCES ЛИТЕРАТУРА

1. Gudmundsson J.T., Anders A., von Keudell A. // *Plasma Sources Sci. Technol.* 2022. V. 31(8). P. 083001. DOI: 10.1088/1361-6595/ac7f53.
2. Golovanov A.V., Luparev N.V., Sorokin B.P. // *Chem-ChemTech* [Izv. Vyssh. Uchebn. Zaved. Khim. Khim. Tekhnol.]. 2020. V. 63, N 11. P. 49–56 (in Russian). DOI: 10.6060/ivkkt.20206311.6232. Голованов А.В., Лупарев Н.В., Сорокин Б.П. // Изв. вузов. Химия и хим. технология. 2020. Т. 63. Вып. 11. С. 49–56. DOI: 10.6060/ivkkt.20206311.6232.
3. Luparev N.V., Sorokin B.P., Aksenenkov V.V. // *Chem-ChemTech* [Izv. Vyssh. Uchebn. Zaved. Khim. Khim. Technol.]. 2020. V. 63, N 12. P. 77–84 (in Russian). DOI: 10.6060/ivkkt.20206312.6312. Лупарев Н.В., Сорокин Б.П., Аксененков В.В. // Изв. вузов. Химия и хим. технология. 2020. Т. 63. Вып. 12. С. 77–84. DOI: 10.6060/ivkkt.20206312.6312.
4. Gudmundsson J.T., Brenning N., Lundin D., Helmersson U. // *J. Vacuum Sci. Technol. A: Vacuum, Surfaces, Films.* 2012. V. 30(3). P. 030801. DOI: 10.1116/1.3691832.
5. Kaziev A.V., Shchelkanov I.A., Khodachenko G.V. // *Proc. SPIE*. 2015. V. 9442. P. 94420J. DOI: 10.1117/12.2086913.
6. Greczynski G., Petrov I., Greene J.E., Hultman L. // *J. Vacuum Sci. Technol. A*. 2019. V. 37(6). P. 060801. DOI: 10.1116/1.5121226.
7. Tumarkin A.V., Kaziev A.V., Kharkov M.M., Kolodko D.V., Il'ychev I.V., Khodachenko G.V. // *Surf. Coat. Technol.* 2016. V. 293. P. 42–47. DOI: 10.1016/j.surfcoat.2015.12.070.
8. Kaziev A.V., Kolodko D.V., Tumarkin A.V., Kharkov M.M., Lisenkov V.Yu., Sergeev N.S. // *Surf. Coat. Technol.* 2021. V. 409. P. 126889. DOI: 10.1016/j.surfcoat.2021.126889.
9. Sidelev D.V., Bleykher G.A., Krivobokov V.P., Koishybayeva Z. // *Surf. Coat. Technol.* 2016. V. 308. P. 168–173. DOI: 10.1016/j.surfcoat.2016.06.096.
10. Tumarkin A.V., Kaziev A.V., Kolodko D.V., Pisarev A.A., Kharkov M.M., Khodachenko G.V. // *Phys. Atomic Nuclei* 2015. V. 78(14). P. 1674–1676. DOI: 10.1134/S1063778815140136.
11. Posadowski W.M. // *Thin Solid Films*. 2004. V. 459(1–2). P. 258–261. DOI: 10.1016/j.tsf.2003.12.106.
12. Sidelev D.V., Krivobokov V.P. // *Vacuum*. 2019. V. 160. P. 418–420. DOI: 10.1016/j.vacuum.2018.12.001.
13. Sidelev D.V., Bleykher G.A., Grudinin V.A. // *Surf. Coat. Technol.* 2018. V. 334. P. 61–70. DOI: 10.1016/j.surfcoat.2017.11.024.
14. Kim H.J. // *Sci. Rep.* 2019. V. 9(1). P. 11555. DOI: 10.1038/s41598-019-47723-2.
15. Chodun R., Wicher B., Nowakowska-Langier K., Minikayev R., Dypa-Uminskaya M., Zdunek K. // *Coatings*. 2022. V. 12(7). P. 1022. DOI: 10.3390/coatings12071022.
16. Sasaki K., Koyama H. // *Appl. Phys. Express*. 2018. V. 11(3). P. 036201. DOI: 10.7567/APEX.11.036201.
17. Moiseev K.M., Nazarenko M.V. // *AIP Conf. Proc.* 2019. V. 2171. P. 170010. DOI: 10.1063/1.5133321.
18. Leonova K., Britun N., Konstantinidis S. // *J. Phys. D: Appl. Phys.* 2022. V. 55(34). P. 345202. DOI: 10.1088/1361-6463/ac72d0.
19. Posadowski W.M., Radzimski Z.J. // *J. Vacuum Sci. Technol. A: Vacuum, Surfaces, Films*. 1993. V. 11(6). P. 2980–2984. DOI: 10.1116/1.578679.
20. Makarova M., Moiseev K., Nazarenko A., Luchnikov P., Dalskaya G., Katakhova N. // *Key Eng. Mater.* 2018. V. 781. P. 8–13. DOI: 10.4028/www.scientific.net/KEM.781.8.
21. Bleykher G.A., Borduleva A.O., Yuryeva A.V. // *Surf. Coat. Technol.* 2017. V. 324. P. 111–120. DOI: 10.1016/j.surfcoat.2017.05.065.
22. Kaziev A.V., Tumarkin A.V., Leonova K.A., Kolodko D.V., Kharkov M.M., Ageychenkov D.G. // *Vacuum*. 2018. V. 156. P. 48–54. DOI: 10.1016/j.vacuum.2018.07.001.
23. Bleykher G.A., Yuryeva A.V., Shabunin A.S., Sidelev D.V., Grudinin V.A., Yuryev Y.N. // *Vacuum*. 2019. V. 169. P. 108914. DOI: 10.1016/j.vacuum.2019.108914.
24. Yurjev Y.N., Kiseleva D.V., Zaitcev D.A., Sidelev D.V., Korneva O.S. // *J. Phys.: Conf. Ser.* 2016. V. 669. P. 012066. DOI: 10.1088/1742-6596/669/1/012066.
25. Sidelev D.V., Bestetti M., Bleykher G.A. // *Surf. Coat. Technol.* 2018. V. 350. P. 560–568. DOI: 10.1016/j.surfcoat.2018.07.047.
26. Tumarkin A., Zibrov M., Khodachenko G., Tumarkina D. // *J. Phys.: Conf. Ser.* 2016. V. 768. P. 012015. DOI: 10.1088/1742-6596/768/1/012015.
27. Strijckmans K., Moens F., Depla D. // *J. Appl. Phys.* 2017. V. 121(8). P. 080901. DOI: 10.1063/1.4976717.
28. Berg S., Särhammar E., Nyberg T. // *Thin Solid Films*. 2014. V. 565. P. 186–192. DOI: 10.1016/j.tsf.2014.02.063.
29. Barybin A.A., Shapovalov V.I. // *J. Appl. Phys.* 2007. V. 101(5). P. 054905. DOI: 10.1063/1.2435795.
30. Chodun R., Dypa M., Wicher B. // *Appl. Surf. Sci.* 2022. V. 574. P. 151597. DOI: 10.1016/j.apsusc.2021.151597.
31. Graillot-Vuillecot R., Thomann A.-L., Lecas T., Cachoncinlle C., Millon E., Caillard A. // *Vacuum*. 2022. V. 197. P. 110813. DOI: 10.1016/j.vacuum.2021.110813.
32. Shapovalov V.I., Zav'yalov A.V., Meleshko A.A. // *Surf. Coat. Technol.* 2021. V. 417. P. 127189. DOI: 10.1016/j.surfcoat.2021.127189.
33. Goncharov A.O., Minzhulina E.A., Shapovalov V.I. // *IOP Conf. Ser.: Mater. Sci. Eng.* 2018. V. 387. P. 012020. DOI: 10.1088/1757-899X/387/1/012020.
34. Shapovalov V.I., Smirnov V.V. // *J. Phys.: Conf. Ser.* 2017. V. 857. P. 012039. DOI: 10.1088/1742-6596/857/1/012039.
35. Kaziev A.V., Kolodko D.V., Sergeev N.S. // *Plasma Sources Sci. Technol.* 2021. V. 30(5). P. 055002. DOI: 10.1088/1361-6595/abf369.

Поступила в редакцию (Received) 26.04.2023  
Принята к опубликованию (Accepted) 21.06.2023